NANO LETTERS

Subscriber access provided by DUKE UNIV

Letter

Three Dimensional Single-Walled Carbon Nanotubes

Jennifer Lu, Dongning Yuan, Jie Liu, Weinan Leng, and Thomas E. Kopley

Nano Lett., **2008**, 8 (10), 3325-3329 • DOI: 10.1021/nl801744z • Publication Date (Web): 05 September 2008

Downloaded from http://pubs.acs.org on January 1, 2009

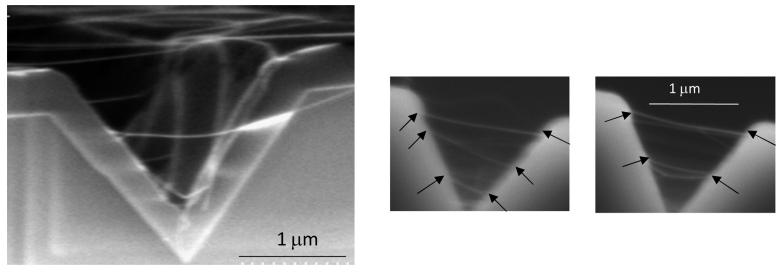

More About This Article

Additional resources and features associated with this article are available within the HTML version:

- Supporting Information
- Access to high resolution figures
- Links to articles and content related to this article
- Copyright permission to reproduce figures and/or text from this article

View the Full Text HTML

ACS Publications
High quality. High impact.

Nano Letters is published by the American Chemical Society. 1155 Sixteenth Street N.W., Washington, DC 20036

NANO LETTERS

2008
Vol. 8, No. 10
3325-3329

Three Dimensional Single-Walled Carbon Nanotubes

Jennifer Lu,*,† Dongning Yuan,‡ Jie Liu,‡ Weinan Leng,† and Thomas E. Kopley§

University of California at Merced, Merced, California, Duke University, Durham, North Carolina, and Agilent Labs, Santa Clara, California

Received June 18, 2008; Revised Manuscript Received August 13, 2008

ABSTRACT

We report a simple fabrication method of creating a three-dimensional single-walled carbon nanotube (CNT) architecture in which suspended CNTs are aligned parallel to each other along the conventionally unused third dimension at lithographically defined locations. Combining top-down lithography with the bottom-up block copolymer self-assembly technique and utilizing the excellent film forming capability of polymeric materials, highly uniform catalyst nanoparticles with an average size of 2.0 nm have been deposited on sidewalls for generating CNTs with 1 nm diameter. This three-dimensional platform is useful for fundamental studies as well as technological exploration. The fabrication method described herein is applicable for the synthesis of other very small 1D nanomaterials using the catalytic vapor deposition technique.

Single-walled carbon nanotubes (SWNTs) have exceptional electronic, optoelectronic, and mechanical properties. They are direct bandgap materials, exhibiting ballistic electron transport properties and exceptionally high current carrying capability.[1−5] Additionally, their bandgap can be tuned by adjusting diameter. Such unique properties have led to the exploration of the use of carbon nanotubes (CNTs) in photonics and electronics.[1,6−13]

A single device element that contains an ensemble of defect-free and electronically isolated semiconducting SWNTs is required for many real-world applications. A device consisting of a large number of tubes provides good device-to-device uniformity, even if the properties of individual tubes are heterogeneous. More importantly, current carrying capability increases with increasing tube density.[13] Thus device performance will be greatly enhanced, leading to, for example, high performance transistors for digital and RF applications. High-density carbon nanotubes are needed for achieving sufficiently high total surface area for light sensing applications. A CNT-based photovoltaic device requires high-density CNTs to efficiently capture light. Analogously, the intensity of infrared light in a CNT-based IR emitter is proportional to the number of tubes. The higher the tube density is, the brighter the emission will be.

Recently, surfaces such as quartz and sapphire have been demonstrated to induce pseudoepitaxial growth of CNTs. This technique, coined nanotube epitaxy, has produced aligned and electronically isolated SWNTs.[14−21] However, the maximum tube density on these two-dimensional surfaces is limited by a combination of the underlying surface structure and the minimum spacing between catalyst nanoparticles, which is limited by nanocatalyst aggregation at high growth temperature. To further increase tube density, we have explored using conventionally untouched "real estate" in the third dimension.

Herein, we report the successful synthesis of suspended SWNTs distributed in a three-dimensional (3D) configuration. Suspended 3D SWNTs, distributed vertically along the depth of a trench, are more or less aligned with their orientations orthogonal to the trench direction. This work is an extension of our previous demonstration of using block copolymers as templates to generate uniform catalyst nanoparticles for synthesizing high-quality SWNTs over a large surface area.[22] Combining top-down lithography with bottom-up block copolymer self-assembly and utilizing the excellent film forming capability of polymeric materials, highly uniform catalyst nanoparticles with an average size of 2.0 nm have been deposited on sloped silicon oxide surfaces formed by the plasma enhanced chemical vapor deposition technique. Suspended, isolated individual SWNTs arranged at spatially predetermined locations have been fabricated. Raman analysis has shown that tube diameter is uniform, around 1.2 nm. The lack of Raman active D-band associated with amorphous carbon and defects suggests that suspended 3D SWNTs are high quality with very low-defect and amorphous carbon content. SWNTs are oriented perpendicular to trench sidewalls as seen in scanning electron microscopy (SEM) images, independent of the gas flow direction, suggesting another way to directly orient tubes during growth. Such a 3D platform is useful for fundamental studies of CNT intrinsic properties and as well as exploration

* To whom correspondence should be addressed.
† University of California at Merced.
‡ Duke University.
§ Agilent Technologies.

10.1021/nl801744z CCC: $40.75 © 2008 American Chemical Society
Published on Web 09/05/2008

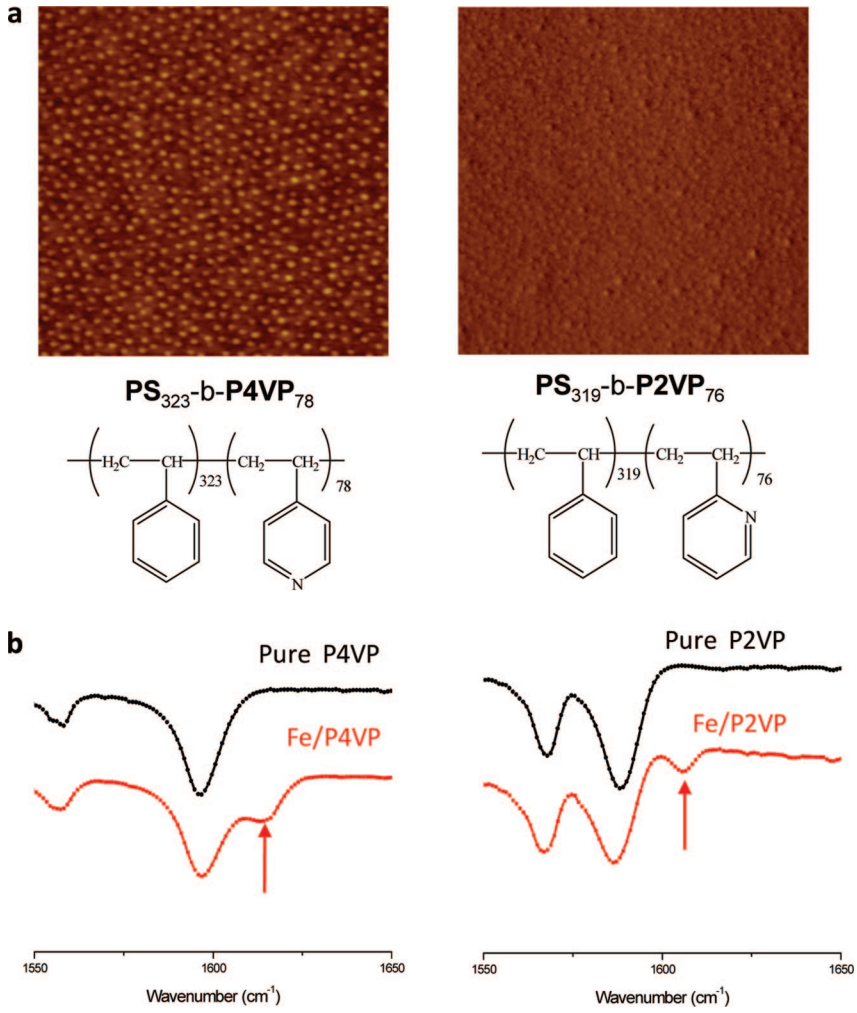

Figure 1. (a) AFM height images (scan area, 1 × 1 μm; height, 5 nm). (b) FTIR spectra with pure P4VP and P2VP with and without addition of $FeCl_2 \cdot 4H_2O$. Spectra was offset for clarification.

of CNT-based unified devices for electronic and optoelectronic applications and CNT-based chemical sensing.

Experimental Results and Discussions. *Iron Nanoparticles Derived from Block Copolymer Templates.* Uniform size catalyst nanoparticles with identical catalytic activity are critical for achieving CNTs with homogeneous properties. Such uniform size catalyst nanoparticles are also the prerequisite for producing high yield CNTs with minimum amorphous carbon. Pyridine-based block copolymers, polystyrene-**b**-poly(2-vinyl pyridine) (PS-**b**-P2VP) and polystyrene-**b**-poly(4-vinylpyridine) (PS-**b**-P4VP), purchased from Polymer Source, were used as templates for the preparation of iron nanoparticles. Iron(II) chloride tetrahydrate from Aldrich was used as the iron precursor. Toluene, purchased from Aldrich, is a solvent preferable to polystyrene.

In this set of experiments, PS_{323}-**b**-$P4VP_{78}$ and PS_{319}-**b**-$P2VP_{76}$ were first dissolved in toluene. Then iron chloride was introduced to yield a 0.25 wt % polymer solution with the molar ratio of iron/pyridyl to be 0.13. After stirring for 24 h at room temperature, these metal precursor-loaded polymer solutions were then spin-coated on patterned silicon oxide surfaces. Finally oxygen plasma was used to remove block copolymer templates. Figure 1 is a set of atomic force microscopy (AFM) height images of surface morphology after oxygen plasma. AFM height analysis was performed on a Veeco Dimension 5000. Iron nanoparticles with an average size of 1.6 nm, according to the AFM height analysis, were derived from using PS_{323}-**b**-$P4VP_{78}$ as the template. Unlike our previous results, the PS_{319}-**b**-$P2VP_{76}$ template was unable to generate nanoparticles.

To determine if iron(II) is capable of forming coordination bonds with pyridine groups, regardless of the location of nitrogen on the pyridine ring, poly(2-vinyl pyridine) (P2VP) and poly(4-vinylpyridine) (P4VP) purchased from Polymer Source was used to study metal complexation ability. Fourier transform IR (FTIR) spectra, displayed in Figure 1b before and after inclusion of iron(II) chloride tetrahydrate, were acquired using a Nicolet MagNA-IR 850. The appearance of new bands at 1616 cm^{-1} and 1603 cm^{-1} in iron-loaded P4VP and P2VP, respectively, are characteristic of pyridine complexes with metals.[22,23] As validated by FTIR analysis, pyridine with its lone pair of electrons on nitrogen can complex with iron(II), a transition metal with unfilled d-orbitals, as indicated in Figure 1b.

Our previous publication shows that due to partial screening of nitrogen in P2VP, PS_{319}-**b**-$P2VP_{76}$ molecules cannot themselves self-assemble in toluene.[24] However, after a sufficient amount of metal is complexed with 2-vinyl pyridine

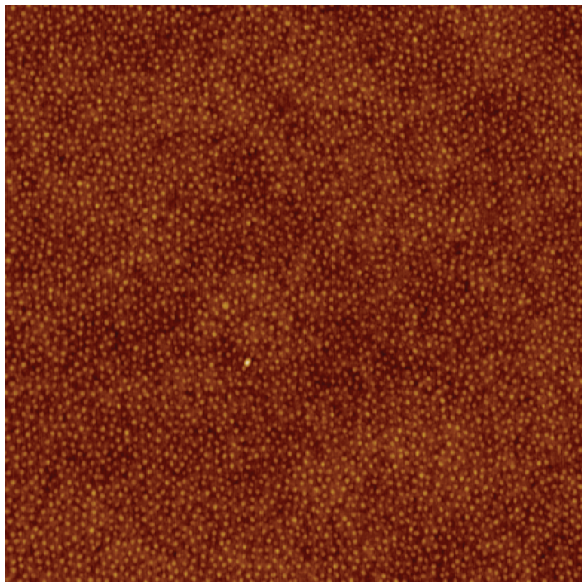

Figure 2. A representative AFM height image of Fe nanoparticles. (scan area, 3 × 3 μm; height, 5 nm)

units, for example, iron(II)/pyridyl = 0.25, the metal-modified P2VP will become hydrophilic enough to induce micellization of PS-**b**-P2VP in toluene. In this investigation, to synthesize CNTs with diameter around 1 nm, iron oxide nanoparticles need to be less than 2.0 nm. Thus the molar ratio of iron(II) to pyridine was adjusted to be around 0.13 accordingly. Statistically, only every seventh 2-vinyl pyridine functional group has iron attached. The absence of nanoparticles on a surface prepared using the iron loaded PS_{319}-**b**-$P2VP_{76}$ solution indicates that P2VP with low iron(II) content is not hydrophilic enough to induce self-assembly in toluene.

On the contrary, the P4VP chain is so polar that micelles of pure PS_{323}-**b**-$P4VP_{78}$ block polymers can be formed in toluene.[24] Despite the tendency of forming intra- and intermolecular bonds between metals and 4-vinylpyridine and the multivalent nature of a polymer system, iron nanoparticles with uniform size have been prepared using the PS_{323}-**b**-$P4VP_{78}$ template. This is probably due to a relatively low stability constant value for the complexation between iron(II) and 4VP, compared to Co(II) or Ni(II) and 4VP. [25,26]

Due to excellent film forming capability of a polymeric material, solution micelles can be distributed evenly on a surface. Figure 2 is an AFM height image demonstrating that uniform-sized iron oxide nanoparticles can be evenly distributed over a large surface area. It is known that high molecular weight polymers have a tendency to form conformal films over topographic surfaces. High molecular weight polyimide precursor, polyamic acid, forms a more conforming coating over topography while low molecular weight oligomer such as Dow Cyclotene tends to planarize a surface with topography. Therefore, it is conceivable that a monolayer of PS_{323}-**b**-$P4VP_{78}$ micelles with iron sequestered in the core can be formed on sloped sidewalls of trenches. This is manifested by uniform diameter CNTs produced using these catalyst nanoparticles on sidewalls. From SEM analysis, the spin-coated film is conforming to the sloped trench sidewall but with a thicker layer in the bottom of the trench. The thicker layer will culminate in a large number of nanocatalysts in close proximity to each other, so they will coalesce and will not be able to initiate CNT growth.

CNT Synthesis and Characterization. Sloped sidewalls were formed by using a one-step patterning process. AZ 1512 photoresist was spin-coated on (100) Si wafers with 100 nm of thermal silicon oxide and then exposed using a Karl-Suss MA-6 mask aligner. Wafers were then subsequently developed by a 0.26N TMAH developer. Wet etching of the silicon dioxide by buffered HF was followed by a Si etch in a hot KOH bath to form sloped trenches. After resist stripping by acetone, buffered HF was employed to remove the 100 nm thermal silicon dioxide. A layer of 50 nm silicon oxide was subsequently deposited using the plasma-enhanced chemical vapor deposition technique to coat the etched trench surface. Finally, iron(II) loaded PS_{323}-**b**-$P4VP_{78}$ micelles were

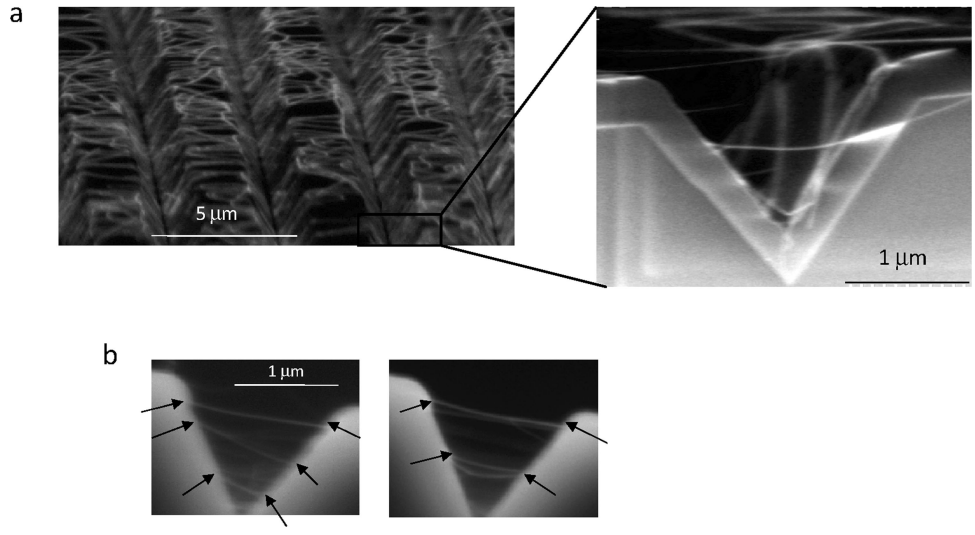

Figure 3. (a) Representative tilted SEM images of substrates after CNT growth. (b) Representative cross-section SEM images after CNT growth. Black arrows pinpoint locations of sidewalls on which CNTs are attached.

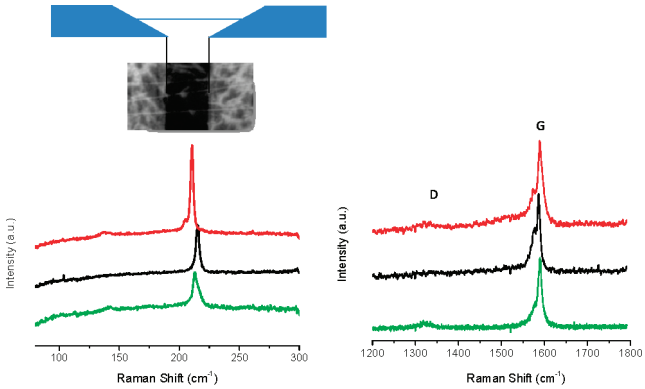

Figure 4. Typical Raman spectra of suspended CNTs at radial breathing region (left) and in-plane graphene oscillation region (right). The inset is a top-down SEM of suspended CNTs used for Raman analysis.

deposited. After stripping the block copolymer template by oxygen plasma, catalyst nanoparticles were formed on the sidewalls of the trenches. The substrate was then treated with oxygen plasma for 15 min followed by CVD growth of SWNTs at 900 °C. First the reduction to iron(0) to activate nanocatalyst was carried out in the home-built growth chamber with a flow of 700 sccm H_2 for 20 min at 700 °C. The temperature was ramped up to 900 °C and held for 5 min before introducing the carbon precursor, which was composed of 800 sccm CH_4 and 20 sccm C_2H_4. After 1 min, the C_2H_4 was turned off and the growth continued for 9 min before switching off the CH_4. The samples were then cooled to room temperature under the protection of H_2 and inspected on a Hitachi S-4500 scanning electron microscope. Raman spectra were obtained with a Jobin-Yvon T64000 triple spectrometer with microprobe sampling (100× objective).

Figure 3a is a representative set of tilted SEM images showing that SWNTs have been formed in between sloped sidewalls. The density of isolated tubes per unit volume has been greatly increased by the structure which consists of suspended and isolated SWNTs in a 3D configuration. Figure 3b is another set of typical SEM images showing CNTs suspended between trench sidewalls. Tubes are more or less parallel to each other, suggesting that surface topography might induce tube alignment. This is the first demonstration of fabricating 3D SWNTs where suspended and isolated pristine CNTs are populated in a spatially predefined 3D configuration.

Suspended SWNTs yield greatly enhanced Raman signals due to the absence of the substrate interaction.[27] They are used for accurate determination of tube diameters. Raman spectra were obtained using an excitation wavelength of 632.8 nm, focused spot size about 1 μm^2, integration time of 750 s, and laser power of 1.0 mW. CNTs show characteristic low-energy peaks in their Raman spectra corresponding to the radial breathing vibrational mode with A_{1g} symmetry. Radial breathing vibration is unique to nanotubes with one or few walls. Since the frequency of the radial breathing mode (RBM) is inversely proportional to CNT diameter, the diameters of CNTs can thus be estimated. Figure 4 shows Raman spectra of several nanotubes. The RBM bands are between 210 to 230 nm indicating that the majority of tubes are around 1 nm in diameter. Such uniform tube diameter is attributed to highly uniform nanocatalysts, derived from the self-assembled polymer micelles. The absence of D band, which is related to amorphous carbon and defects, indicates that high quality, defect-free SWNTs have been fabricated in spatially controlled three-dimensional locations.

To demonstrate that tube orientation is induced by surface topography, suspended CNTs have been synthesized from patterned surfaces with neighboring trenches oriented perpendicularly as shown in the optical image in Figure 5. The tilted SEM images are 3D CNTs grown in these trenches. It can be seen that suspended CNTs are oriented orthogonally to the sidewalls of trenches and are more or less parallel with each other. CNTs could grow randomly in any direction without discretion. A small portion of tubes grow on plateaus as can be seen clearly from the SEM images in Figure 5. However, only tubes with proper orientation can grow across a trench. The shorter the distance is, the more likely it is that CNTs will grow from one sidewall and reach the opposite sidewall surface. During CNT synthesis, their ends grow until they touch the opposite sidewall. CNTs with their orientation perpendicular to a trench have the shortest suspension length or travel distance, therefore are more likely to occur. This result suggests that surface topography can be employed to control tube orientation. By combining this effect with other methods such as carbon precursor gas flow

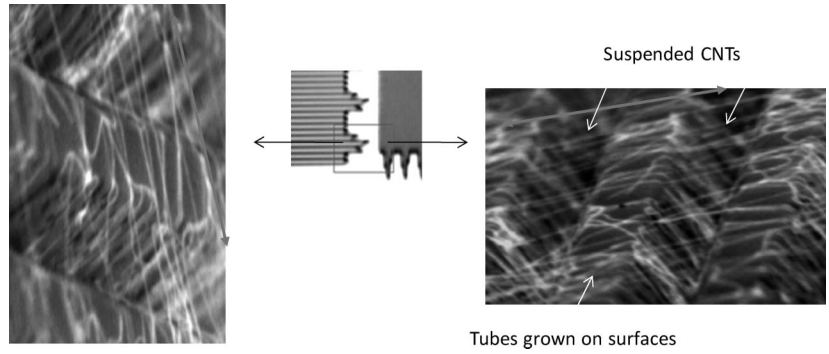

Figure 5. Tilted SEM images (3 μm × 2 μm field of view) showing that suspended SWNTs aligned orthogonally to trench orientation (left and right). The optical image (center) shows that this set of trenches are in close proximity, oriented 90° with respect to each other. Blue arrows in the images indicate tube orientations that are approximately perpendicular to trench orientation.

direction, it is expected that tube orientation control can be further improved. More systematic work is underway to understand this phenomenon.

Conclusion. Using the block copolymer approach, uniform catalyst nanoparticles with size less than 2 nm have been synthesized. Due to excellent film forming capability of a polymeric material, the block copolymer approach allows uniform distribution of micelles, parents of nanocatalysts, on trench sidewall surfaces. SWNTs with narrow size distribution have been successfully synthesized, suspended over trenches with tubes parallel to each other, forming a unique 3D structure. Using this method, high density and electronically isolated suspended SWNTs with controlled spatial arrangement can be fabricated. Additionally, it has been found that low-temperature PECVD silicon oxide is a good catalyst support for CNT growth. This method is applicable for synthesizing a variety of other 1D nanomaterials using the catalytic chemical vapor deposition technique.

Unlike solution-based SWNT suspensions, suspended and undisturbed pristine SWNTs are ideal candidates for fundamental study of intrinsic CNT properties. Suspended tubes, which eliminate the nonradiative recombination channel resulting from the interaction of CNTs with substrates, are superb photon absorbing materials.[28] The incorporation of 3D suspended SWNTs in a single device can greatly increase fill factor and thus open a new pathway for exploration of SWNTs in optoelectronics: near-infrared detectors and photovoltaic devices. Conversely, extremely bright tunable IR emitters can be fabricated using this platform. This approach of generating isolated tubes eliminates the need for surfactants, which block sites for functionalization, and aggressive sonication, which damages the tubes. This 3D suspended CNT platform can also be used for optical-based sensing by detecting the change of fluorescence emission content. Furthermore, this new 3D structure with increased tube density using the unexplored real estate along the thickness of a substrate will further increase device drive current and reduce the effect of parasitic capacitance, thus enabling CNT-based electronic devices.

Acknowledgment. We thank Professor Anne Myers Kelley for providing the Jobin-Yvon Raman spectrometer and Young Yim at Agilent Technologies for silicon wafer processing.

References

(1) Javey, A.; Guo, J.; Wang, Q.; Lundstrom, M.; Dai, H. J. Ballistic Carbon Nanotube Field-effect Transistors. *Nature* **2003**, *424*, 654–657.
(2) Moon, S. Y.; Song, W.; Kim, N.; Lee, J. S.; Na, P. S.; Lee, S. G.; Park, J. W.; Jung, M. H.; Lee, H. W.; Kang, K.; Lee, C. J.; Kim, J. Current-carrying Capacity of Double-wall Carbon Nanotubes. *Nanotechnology* **2007**, *18*, 235201.
(3) Dresselhaus, M. S.; Dresselhaus, G.; Avouris, P. *Carbon Nanotubes*; Springer: Berlin, 2001..
(4) Misewich, J. A.; Martel, R.; Avouris, P.; Tsang, J. C.; Heinze, S.; Tersoff, J. Electrically Induced Optical Emission from a Carbon Nanotube FET. *Science* **2003**, *300*, 783–786.
(5) Saito, R.; Dresselhaus, G.; Dresselhaus, M. S. *Physical Properties of Carbon Nanotubes*; Imperial College: London, 1998..
(6) Barone, P. W.; Baik, S.; Heller, D. A.; Strano, M. S. Near-infrared Optical Sensors Based on Single-Walled Carbon Nanotubes. *Nat. Mater.* **2005**, *4*, 86–92.
(7) Snow, E. S.; Perkins, F. K.; Houser, E. J.; Badescu, S. C.; Reinecke, T. L. Chemical Detection with a Single-Walled Carbon Nanotube Capacitor. *Science* **2005**, *307*, 1942–1945.
(8) Itkis, M. E.; Borondics, F.; Yu, A. P.; Haddon, R. C. Bolometric Infrared Photoresponse of Suspended Single-Walled Carbon Nanotube Films. *Science* **2006**, *312* (5772), 413–416.
(9) Freitag, M.; Martin, Y.; Misewich, J. A.; Martel, R.; Avouris, P. Photoconductivity of Single Carbon Nanotubes. *Nano Lett.* **2003**, *3*, 1067–1071.
(10) Lee, J. U. Photovoltaic Effect in Ideal Carbon Nanotube Diodes. *Appl. Phys. Lett.* **2005**, *87*, 073101.
(11) Wei, J. Q.; Jia, Y.; Shu, Q. K.; Gu, Z. Y.; Wang, K. L.; Zhuang, D. M.; Zhang, G.; Wang, Z. C.; Luo, J. B.; Cao, A. Y.; Wu, D. H. Double-Walled Carbon Nanotube Solar Cells. *Nano Lett.* **2007**, *7*, 2317–2321.
(12) Chen, J.; Perebeinos, V.; Freitag, M.; Tsang, J.; Fu, Q.; Liu, J.; Avouris, P. Bright Infrared Emission from Electrically Induced Excitons in Carbon Nanotubes. *Science* **2005**, *310* (5751), 1171–1174.
(13) Kang, S. J.; Kocabas, C.; Ozel, T.; Shim, M.; Pimparkar, N.; Alam, M. A.; Rotkin, S. V.; Rogers, J. A. High-performance electronics using dense, perfectly aligned arrays of single-walled carbon nanotubes. *Nat. Nanotechnol.* **2007**, *2*, 230–236.
(14) Ding, L.; Yuan, D.; Liu, J. Growth of High-Density Parallel Arrays of Long Single-Walled Carbon Nanotubes on Quartz Substrates. *J. Am. Chem. Soc.* **2008**, *130*, 5428–5429.
(15) Ismach, A.; Kantorovich, D.; Joselevich, E. Carbon Nanotube Graphoepitaxy: Highly Oriented Growth by Faceted Nanosteps. *J. Am. Chem. Soc.* **2005**, (127), 11554–11555.
(16) Han, S.; Liu, X.; Zhou, C. Template-Free Directional Growth of Single-Walled Carbon Nanotubes on a- and r- Plane Sapphire. *J. Am. Chem. Soc.* **2005**, *127*, 5294–5295.
(17) Ismach, A.; Segev, L.; Wachtel, E.; Joselevich, E. Atomic-step-templated formation of single wall carbon nanotube patterns. *Angew. Chem., Int. Ed.* **2004**, *43*, 6140–6143.
(18) Ismach, A.; Kantorovich, D.; Joselevich, E. Carbon nanotube graphoepitaxy: Highly oriented growth by faceted nanosteps. *J. Am. Chem. Soc.* **2005**, *127*, 11554–11555.
(19) Ago, H.; Nakamura, K.; Ikeda, K.; Uehara, N.; Ishigami, N. Aligned growth of isolated single-walled carbon nanotubes programmed by atomic arrangement of substrate surface. *Chem. Phys. Lett.* **2005**, *408*, 433–438.
(20) Kocabas, C.; Hur, S.-H.; Gaur, A.; Meitl, M. A.; Shim, M.; Rogers, J. A. Guided growth of large-scale, horizontally aligned arrays of single-walled carbon nanotubes and their use in thin-film transistors. *Small* **2005**, *1*, 1110–1116.
(21) Ismach, A.; Joselevich, E. Orthogonal self-assembly of carbon nanotube crossbar architectures by simultaneous graphoepitaxy and field-directed growth. *Nano Lett.* **2006**, *6*, 1706–1710.
(22) Liu, M.; Yan, X.; Liu, H.; Yu, W. An investigation of the interaction between polyvinylpyrrolidone and metal cations. *React. Funct. Polym.* **2000**, *44*, 55–64.
(23) Bekturov, E. A.; Kudaibergenov, S. E.; Kanapyanova, G. S.; Saltbaeva, S. S.; Skushnikova, A. I.; Pavlova, A. L.; Domnina, E. S. Mössbauer Spectroscopic Studies of Complexes of Fe(III) with Nitrogen Containing Polymers. *Polym J.* **1991**, *23* (4), 339–342.
(24) Lu, J. Nanocatalysts with Tunable Properties Derived from PS-b-PVP Polymer Templates for CNT Synthesis. *J. Phys. Chem. C* **2008**, *112*, 10344–10351.
(25) Kurihara, M. Complexation of Cobalt(II), Nickel(II), and Copper(II) ions with Pyridine, 2-methylpyridine, 3-methylpyridine, and 4-methylpyridine in Acetonitrile. *Z. Naturforsch., B: Chem. Sci.* **2000**, *55*, 277–284.
(26) Hogfeldt, E. *Stability Constants of Metal–Ion Complexes*; Pergamon Press: Oxford, 1982.
(27) Lu, J.; Kopley, T.; Dutton, D.; Liu, J.; Qian,C.; Son, H.; Dresselhaus, M.; Kong, J. Generating suspended single-walled carbon nanotubes across a large surface area via patterning self-assembled catalyst-containing block copolymer thin films. *J. Phys. Chem. B* **2006**, *110* (22), 10585–10589.
(28) Yang, Z.; Ci, L.; Bur, J. A.; Lin, S; Ajayan, P. M. Experimental Observation of an Extremely Dark Material Made By a Low-Density Nanotube Array. *Nano Lett.* **2008**, *8* (2), 446–451.

NL801744Z